Mitochondrial function in the yeast form of the pathogenic fungus *Paracoccidioides brasiliensis*

Vicente P. Martins · Frederico M. Soriani ·
Taisa Magnani · Valéria G. Tudella ·
Gustavo H. Goldman · Carlos Curti ·
Sérgio A. Uyemura

Abstract Differences between the respiratory chain of the fungus *Paracoccidioides brasiliensis* and its mammalian host are reported. Respiration, membrane potential, and oxidative phosphorylation in mitochondria from *P. brasiliensis* spheroplasts were evaluated *in situ*, and the presence of a complete (Complex I–V) functional respiratory chain was demonstrated. In succinate-energized mitochondria, ADP induced a transition from resting to phosphorylating respiration. The presence of an alternative NADH–ubiquinone oxidoreductase was indicated by: (i) the ability to oxidize exogenous NADH and (ii) the lack of sensitivity to rotenone and presence of sensitivity to flavone. Malate/NAD^+-supported respiration suggested the presence of either a mitochondrial pyridine transporter or a glyoxylate pathway contributing to NADH and/or succinate production. Partial sensitivity of NADH/succinate-supported respiration to antimycin A and cyanide, as well as sensitivity to benzohydroxamic acids, suggested the presence of an alternative oxidase in the yeast form of the fungus. An increase in activity and gene expression of the alternative NADH dehydrogenase throughout the yeast's exponential growth phase was observed. This increase was coupled with a decrease in Complex I activity and gene expression of its subunit 6. These results support the existence of alternative respiratory chain pathways in addition to Complex I, as well as the utilization of NADH-linked substrates by *P. brasiliensis*. These specific components of the respiratory chain could be useful for further research and development of pharmacological agents against the fungus.

Keywords *Paracoccidioides brasiliensis* · Mitochondria · Respiratory chain · Alternative pathways

V. P. Martins · F. M. Soriani · T. Magnani · V. G. Tudella · S. A. Uyemura (✉)
Departamento de Análises Clínicas, Toxicológicas e Bromatológicas, Faculdade de Ciências Farmacêuticas de Ribeirão Preto, Universidade de São Paulo,
Av. Café, s/n,
14040-903 Ribeirão Preto, São Paulo, Brazil
e-mail: suyemura@fcfrp.usp.br

G. H. Goldman
Departamento de Ciências Farmacêuticas, Faculdade de Ciências Farmacêuticas de Ribeirão Preto, Universidade de São Paulo,
Av. Café, s/n,
14040-903 Ribeirão Preto, São Paulo, Brazil

C. Curti
Departamento de Física e Química, Faculdade de Ciências Farmacêuticas de Ribeirão Preto, Universidade de São Paulo,
Av. Café, s/n,
14040-903 Ribeirão Preto, São Paulo, Brazil

Abbreviations

SUCC	Succinate
OLIGO	Oligomycin
FCCP	Carbonyl cyanide *p*-trifluoromethoxyphenyl-hydrazone
TMPD/	*N,N,N′,N′*-tetramethyl-*p*-phenylenediamine/
ASC	ascorbate
Ant. A	Antimycin A
KCN	Potassium cyanide
SHAM	Salicylhydroxamic acid
GLUT	Glutamate
MAL	Malate
ROT	Rotenone
FLAV	Flavone
FAM	6-carboxyfluorescein
nd6	Complex I subunit 6 gene
ndh2	Alternative NADH dehydrogenase gene
AOX	Alternative oxidase

Introduction

Paracoccidioides brasiliensis, a thermally dimorphic fungus, is the etiological agent of paracoccidioidomycosis (PMC), the most prevalent human systemic mycosis in Latin America (Restrepo 1985; Brummer et al. 1993), affecting almost ten million individuals (Restrepo et al. 2001; Moreira et al. 2004). It is acquired by inhalation of airborne microconidia, which reach the pulmonary alveolar epithelium and transforms into the parasitic yeast form (Restrepo 1985; Restrepo et al. 2001; San-Blas et al. 2002). The human form of PCM caused by this fungus is characterized by a range of clinical manifestations, from benign or asymptomatic forms to severe and disseminated disease that is often fatal (Ramos and Saraiva 2008). There are two clinical forms of PMC: the acute/subacute form (juvenile type) and the chronic adult form. The juvenile form is characterized by a rapid course and by marked involvement of the reticuloendothelial system and dissemination to multiple host organs (Franco 1987) such as the spleen, liver, lymph nodes and bone marrow. The chronic form represents more than 90% of cases, mostly in adult males, progresses slowly and can take months to years to complete establishment. Unlike the symptoms of the acute form, pulmonary manifestations and respiratory symptoms are nonspecific and include cough, expectoration, and shortness of breath, weight loss, fever and anorexia (Brummer et al. 1993). Usually, there is formation of fibrosis sequelae in the affected organs that may interfere with wellness of the patient.

During infection, thermodimorphic fungi such as *Histoplasma capsulatum, Blastomyces dermatitidis*, and *P. brasiliensis* differentiate into a pathogenic yeast form, a transition that can also be induced (*in vitro*) by temperature changes from room temperature (23–26°C) to 35–37°C. In addition, these pathogens are subjected to significant environmental stress, including exposure to reactive oxygen (ROS) and nitrogen species (RNS) produced by host cells (Moreira et al. 2004; Johnson et al. 2003; Brummer et al. 1989). Elevated sub lethal temperatures (thermal stress or heat shock) probably increase oxidative damage in microbial cells by stimulating ROS generation.

Mitochondria are the main intracellular source of ROS, which are apparently generated at the level of Complexes I and III of the respiratory chain and are able to damage biomolecules like nucleic acids, lipids, and proteins (Harman 1956, 1981, 1998). To control ROS, cells have developed diverse detoxification mechanisms, including superoxide dismutase, catalase, the gluthatione/thioredoxin system, and uncoupling proteins (Jezek and Hlavata 2005). In addition to proton-pumping complexes, the mitochondrial respiratory chain of plants and fungi contains alternative pathways, mainly NADH–ubiquinone oxidoreductases and ubiquinol oxidases that prevent ROS generation (Joseph-Horne et al. 2001). Alternative NADH–ubiquinone oxidoreductases could be located in the matrix space of mitochondria, oxidizing internal NADH, or alternatively in the intermembrane space, where they could oxidize cytosolic NADH and/or NADPH [for a review see (Kerscher 2000)]. Ubiquinol oxidases (cyanide-resistant oxidases) directly transfer electrons from ubiquinol to oxygen. Both pathways bypass the proton-pumping complexes, impairing electron transfer from proton translocation. Alternative oxidases (AOX) have been documented in plants (Siedow and Umbach 1995; Vanlerberghe and McIntosh 1997; Borecky and Vercesi 2005), algae (Tischner et al. 2004), yeasts (Veiga et al. 2003), free-living amoebae (Jarmuszkiewicz et al. 2002), and protozoa (Suzuki et al. 2005), as well as pathogenic fungi such as *Aspergillus fumigatus* (Tudella et al. 2004), *H. capsulatum* (Johnson et al. 2003), and *P. brasiliensis* (Goldman et al. 2003; Marques et al. 2004).

Most current information on mitochondria from *P. brasiliensis* comes from studies on *H. capsulatum* (Maresca et al. 1981) or on the mycelial-yeast phase transition of *P. brasiliensis* (Medoff et al. 1987). These studies, however, demonstrate neither oxidative phosphorylation activity nor an ability to sustain a mitochondrial membrane potential. We therefore address the mitochondrial energetic function of *P. brasiliensis* to aid future studies attempting to elucidate targets of pharmacological potential. Furthermore, the presence of alternative respiratory chain pathways and the use of NADH as a respiratory substrate have not previously been demonstrated in *P. brasiliensis*.

Materials and methods

Chemicals

ADP, AMP, antimycin A, ascorbate, benzohydroxamic acid (BHAM), bovine serum albumin (BSA), carbonyl cyanide *p*-trifluoromethoxyphenylhydrazone (FCCP), dimethyl sulfoxide (DMSO), dithiotreitol (DTT), ethyleneglycol-bis-(β-amino ethyl ether)-*N,N,N′,N′*-tetra acetic acid (EGTA), flavone, GTP, nicotinamide adenine dinucleotide oxidized form (NAD$^+$), nicotinamide adenine dinucleotide reduced form (NADH), oligomycin, KCN, rotenone, salicylhydroxamic acid (SHAM), *N,N,N′,N′*-tetramethyl-*p*-phenylenediamine (TMPD), and valinomycin were purchased from Sigma (St Louis, MO, USA). All other reagents were analytical grade. All aqueous stock solutions were prepared using glass-distilled deionized water, except water-insoluble compounds that were prepared in DMSO or absolute ethanol from Merck (Darmstadt, Germany).

Strains and culture conditions

The *P. brasiliensis* isolate 18 was maintained in the mycelium form in solid Sabouraud medium (Difco) at room temperature and in the yeast form in solid PGY medium [0.5% (*w/v*) peptone, 1% (*w/v*) glucose, 0.5% (*w/v*) yeast extract and 1.7% (*w/v*) agar], at 35.5°C. The routine cultivation of *P. brasiliensis* yeast cells for spheroplasts preparation and RNA isolation was performed in liquid PGY medium under rotary shaker aeration, at 35.5°C (San-Blas et al. 1994).

Spheroplasts preparation

Spheroplasts of *P. brasiliensis* were produced from yeast cells at exponential (48–120 h) and stationary (120–240 h) growth stage. Cells were harvested by centrifugation of 150 ml of culture media, washed with cold PBS, and pre-incubated for 1 h at 37°C with shaking at 100 rpm/min in media containing 0.7 M sucrose, 30 mM DTT, and 100 mM Tris-HCl, pH 6.5. After this pre-treatment, cells were harvested and washed twice with digestion buffer containing 0.7 mM sucrose and 50 mM Tris-HCl, pH 6.5. Yeast cell wall digestion was accomplished in 10 ml of digestion buffer containing 35 mg Glucanex® (Novo Nordisk) per gram of wet cells, for 5 h at 37°C, with shaking at 100 rpm. The digestion was stopped by addition of an equal volume of cold digestion buffer, and the spheroplasts were washed twice with the same buffer. The suspension was centrifuged in a swing bucket rotor (Eppendorf centrifuge model 5810 R) at $2,000 \times g$ for 10 min, at 4°C, and the spheroplasts were maintained on ice until use.

Oxygen uptake measurements

Oxygen uptake was measured with a Clark-type electrode (Tudella et al. 2004) fitted to a Gilson oxygraph (Gilson Medical Electronics, Inc., Middleton, WI) in 1.8 ml of standard incubation medium containing 0.6 mM sucrose, 10 mM Hepes-KOH, pH 7.2, 5 mM $MgCl_2$, 2 mM KCl, and 0.5 mM EGTA, at 30°C. The initial solubility of oxygen in the reaction buffer was considered to be 445 ng atoms of O/mL (Helmerhorst et al. 2002). Further additions are indicated in the figure legends. The addition of DMSO in the yeast respiration assays did not influence the oxygen uptake (data not shown). Respiratory parameters were determined as previously described (Chance and Williams 1956).

Determination of mitochondrial membrane potential ($\Delta\psi$)

The mitochondrial membrane potential was determined in *P. brasiliensis* spheroplasts by measuring the fluorescence of safranine O (Petrussa et al. 1992) using a Hitachi F-4500 fluorescence spectrophotometer at 30°C. The excitation and emission wavelengths were respectively 495 and 586 nm; the slit width was 5 nm. To guarantee that the effects observed were due to the exogenous substrates, spheroplasts were depleted of endogenous substrates by incubation for 1–2 h at 4°C. The valinomycin-induced K^+ diffusion potential was used to perform a calibration curve in potassium-free media containing 0.6 M sucrose, 10 mM Na^+-HEPES buffer, pH 7.2, 5 mM $MgCl_2$, 2.0 mM sodium phosphate, and 0.5 mM EGTA. Energized mitochondria were incubated with safranine O in presence of valinomycin and titrated with K^+. The decay caused by the electrogenic influx of cations, as determined by the Nernst equation (Akerman and Wikstrom 1976), assuming intra-mitochondrial $[K^+]$ to be 120 mM, is correlated to the increase in the fluorescence intensity of the dye as it is released from mitochondria (Kowaltowski et al. 2002). Other additions are indicated in the figure legends. Each experiment (oxygen uptake and membrane potential measurements) was repeated at least three times with different preparations, and the figures show representative experiments.

RNA isolation

Yeast cells were disrupted with glass beads and by grinding in liquid nitrogen (Goldman et al. 2003), and immediately mixed with Trizol (Invitrogen) for RNA extraction following the supplier's recommendations. To verify the RNA integrity, 20 µg of RNA from each time point was fractionated in 2.2% of formaldehyde, run on a 1.2% agarose gel, stained with ethidium bromide, and visualized with UV light. The presence of intact 28S and 18S rRNA bands was used as a criterion to verify that the RNA was intact. RNase-free DNase treatment was done in a final volume of 100 µL containing 40 mM Tris-HCl (pH 7.5) and 6 mM $MgCl_2$, 1 µL of RNase-out (Invitrogen), 2.5 µL of 200 mM DTT, and 10 µg of total RNA. The reaction was incubated for 60 min at 37°C and stopped by incubation at 70°C for 30 min. The absence of DNA contamination after the RNase treatment was verified by Real-time PCR quantization of the *P. brasiliensis* α-tubulin gene Ptub1 (http://143.107.203.68/pbver2/default.html) using oligonucleotides forward 5′-ACC CAGCTTGGAAACAGTGCT-3′ and reverse 5′-CACGGACCATCAGCCTTCAAACC [FAM]G-3′.

Real-time PCRs and RT-PCRs

All the real-time PCRs and RT-PCRs were performed using an ABI Prism 7700 sequence detection system (Perkin-Elmer Applied Biosystems). TaqMan EZ RT-PCR kits (Applied Biosystems) were used for RT-PCRs. The ther-

mocycling conditions comprised an initial step at 50°C for 2 min followed by 30 min at 60°C for reverse transcription, 95°C for 5 min, and 40 cycles of 94°C for 20 s and 60°C for 1 min. TaqMan PCR reagent kits were used for PCRs. The thermocycling conditions comprised an initial step at 50°C for 2 min followed by 10 min at 95°C and 40 cycles of 95°C for 15 s and 60°C for 1 min (Semighini et al. 2002). All the *P. brasiliensis* real-time PCR products yielded a single band with the expected size as visualized on agarose gels (data not shown). Since there is no ideal control for gene expression, we first compared the α-tubulin and hexokinase gene probes as normalizers for the expression of these genes. No difference was observed between the two normalizers. Accordingly, the α-tubulin gene was used to normalize all expression results (data not shown). Real-time PCR quantification of the *ndh*2 (accession number CN240857) and *nd*6 (AY268589) genes was done using, respectively, the oligonucleotides forward 5′-CTGGCGGAGAATGTTCCTGAT-3′, reverse 5′-CGGTGTCTCCCGTCCTGTACCAC[FAM]G-3′ and forward 5′-GCAGGAGGACCACTCGC TATG-3′, reverse 5′-CGGTTAGCTCTCC TGGCAGAAAC[FAM]G-3′.

Results

Respiration and oxidative phosphorylation of mitochondria of *P. brasiliensis* spheroplasts

Addition of 10 mM succinate to a suspension of exponentially (60 h) growing *P. brasiliensis* spheroplasts incubated in standard media produced an increase in the rate of oxygen uptake, indicating that the plasma membrane had become permeable to the respiratory substrate (Fig. 1). Subsequent addition of ADP induced a transition in respiration from resting state (i.e., state 4) to phosphorylating state (state 3). This transition was reversed by the addition of 4 μg oligomycin. FCCP at the relatively high concentration of 25 μM, stimulated state 4 respiration, which was partly inhibited by 0.5 μM antimycin A. Addition of the exogenous respiratory substrate TPMD/ascorbate, which reduces the respiratory chain complex IV, restarted respiration that was partially inhibited by KCN. Similar results (not shown) were obtained when succinate was replaced by NADH. Glutamate, malate, citrate, pyruvate, and α-ketoglutarate are usually employed to demonstrate the presence of NADH–ubiquinone oxidoreductase (Complex I) in mitochondria. Isolated, these substrates failed to stimulate ADP phosphorylation during the exponential growth phase of the fungus, but, when added together they increased oxygen uptake and ADP phosphorylation. Endogenous substrates or the potential flavoprotein-linked substrates α-glycerol-3-phosphate or
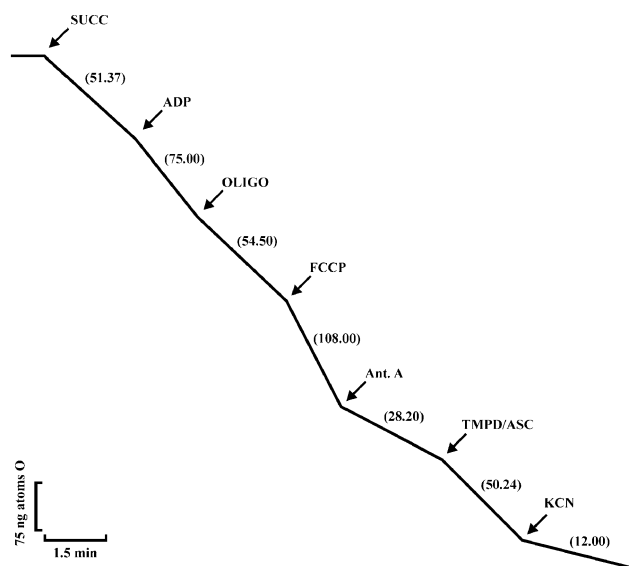

Fig. 1 Oxygen uptake by *P. brasiliensis* spheroplasts. Spheroplasts of *P. brasiliensis* (5×10^6 cells per ml) were incubated at 30°C in 1.8 ml of standard incubation media, as described in experimental procedures. At the times indicated by *arrows*, succinate (10 mM), ADP (2 μmol), oligomycin (4 μg), FCCP (25 μM), antimycin A (0.5 μg), TMPD/ascorbate (300 μM /0.5 mM), or KCN (1 mM), were added. An oxidizable substrate cocktail containing malate (10 mM), glutamate (10 mM), citrate (10 mM), pyruvate (10 mM), and α-ketoglutarate (10 mM), caused a slight oxygen uptake (see Table 1). The same substrates in isolation, α-glycerol-3-phosphate (10 mM) or dihydroorotate (10 mM), did not cause oxygen uptake. However, malate/NAD$^+$ (10 mM/2 mM) did cause oxygen uptake (see also Table 1). The *values in parentheses* represent the rate of oxygen uptake and were expressed as ng atoms O/min/5×10^6 cells/ml. *Graphs* are representative of at least three independent assays

dihydroorotate were not able to stimulate ADP phosphorylation (Table 1).

KCN-resistant respiration of *P. brasiliensis* spheroplasts

The partial inhibition of TMPD/ascorbate-supported respiration by KCN (Fig. 1) suggests the presence of an alternative oxidase in *P. brasiliensis*. To rule out the participation of ascorbate autoxidation in the residual respiration observed following KCN addition, a similar assay, but in the absence of TMPD/ascorbate, was performed. Partial inhibition of succinate- (not shown) or NADH- supported respiration by antimycin A or KCN was relieved by GMP or AMP but was inhibited by SHAM or BHAM (Fig. 2a). GMP or AMP did not stimulate respiration in the presence of SHAM or BHAM (Fig. 2b).

Exogenous NADH oxidation by *P. brasiliensis* spheroplasts

In contrast to mammalian mitochondria, both respiration and ADP phosphorylation in mitochondria of *P. brasiliensis* spheroplasts were stimulated by exogenous NADH. Respi-

Table 1 Substrate oxidation and oxygen uptake by *P. brasiliensis* spheroplasts

Substrates	Rate of respiration (ng atoms of oxygen per min per 5×10^6 cells per ml)	
	State 3	State 4
Substrate cocktail[a]	74.8 ± 2.0[d]	63.7 ± 1.4
NADH	55.2 ± 4.8	43.9 ± 3.3
Succinate	53.5 ± 2.9	44.2 ± 4.5
NADH/Succinate	72.3 ± 2.7	51.4 ± 0.5
Substrate cocktail without NADH	64.1 ± 6.5	48.9 ± 8.3
TMPD/ascorbate	37.8 ± 2.2	37.8 ± 2.2
Complex I substrates cocktail[b]	19.8 ± 1.6	13.55 ± 0.2
Malate	n.d.	n.d.
Malate/NAD^{+}	27.2 ± 1.3	20.5 ± 2.3
Flavoprotein-linked substrates[c]	n.d.	n.d.

Experimental conditions are described in legend of Fig. 1.
n.d. Not detected
[a] Malate, glutamate, citrate, pyruvate, α-ketoglutarate, succinate and NADH
[b] Malate, glutamate, citrate, pyruvate and α-ketoglutarate
[c] α-glycerol-3-phosphate, dihydroorotate
[d] Mean ± S.E.M. values of three determinations in independent assays

ration elicited by a substrate cocktail containing NADH, malate, and glutamate was insensitive to rotenone, even at very high (40 μM) concentrations. Respiration was inhibited, however, by flavone (0.5 mM) added either prior to (Fig. 3a) or after (Fig. 3b) rotenone.

Mitochondrial membrane potential (ΔΨ)

Membrane potential (ΔΨ) is a very sensitive indicator of the mitochondrial energy-coupling condition. Safranin is a lipophilic cation that accumulates in the inner mitochondrial membrane, reducing the fluorescence of the suspension in a manner proportional to the negative charge of the mitochondrial matrix (Akerman and Wikstrom 1976). Thus, safranin fluorescence traces measure only changes in charge across the inner membrane and are insensitive to the second component of the mitochondrial H^{+} gradient, the ΔpH (Kowaltowski et al. 2002). The fluorescence shift is correlated to the membrane potential up to at least 170 mV, and is monitored by fluorescent emissions at 586 nm, when excited at 495 nm. During exponential growth, addition of respiratory substrate to a suspension of *P. brasiliensis* spheroplasts incubated in standard media was followed by a large decrease in fluorescence, with no further change after 6 min (Fig. 4). Addition of ADP caused a small increase in fluorescence, compatible with the utilization of the electrochemical proton potential to drive ADP phosphorylation by ATP synthase (complex V) (Akerman and Wikstrom 1976).

This increase in fluorescence was fully inhibited by the ATP synthase-inhibitor oligomycin. Addition of FCCP or KCN promoted a rapid increase in fluorescence, compatible with depolarization of the inner mitochondrial membrane and return of safranine O to the water phase (Fig. 4, *c*). All other substrates, when tested alone, were unable to generate a Δψ (Fig. 4, *a*), with the exception of malate plus NAD^{+} (Fig. 4, *b*). Based on the extent of the calibrated safranine O shift, the magnitude of the Δψ of mitochondria respiring in either succinate or NADH was ~140 mV (results not shown).

Complex I and alternative NADH dehydrogenase activities during different cellular growth stages

Following a 60 h growth period of the fungus, mitochondrial Δψ in the presence of the Complex I-substrate cocktail plus 2 mM NAD^{+} (Table 1) was slightly inhibited by flavone (Fig. 5a—*a*). A complete inhibition was observed after addition of rotenone. When rotenone was added previously to flavone (Fig. 5a—*b*) a higher inhibition
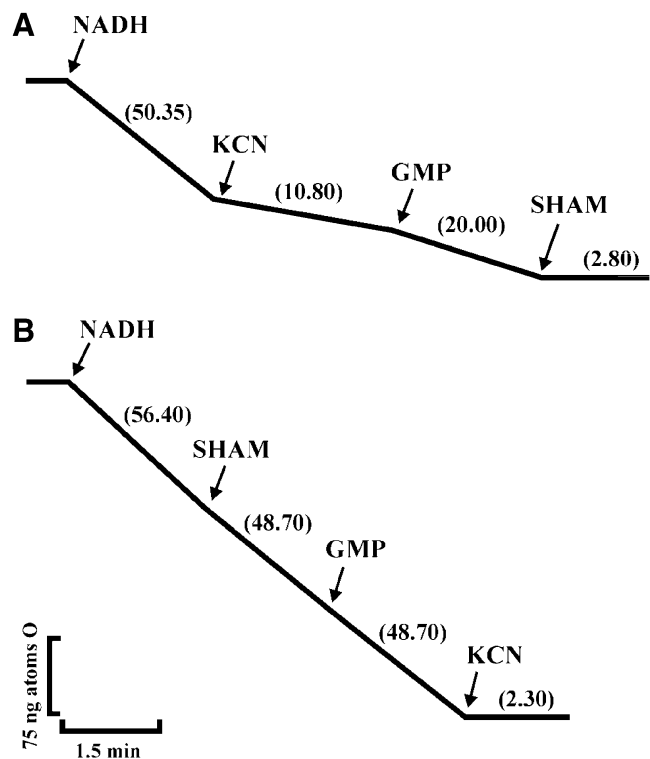

Fig. 2 KCN-resistant respiration in *P. brasiliensis* spheroplasts. **a, b** Spheroplasts of *P. brasiliensis* (5×10^6 cells per ml) were incubated at 30°C in 1.8 ml of standard incubation media. At the times indicated by *arrows*, NADH (2 mM), KCN (1 mM) or antimycin A (0.5 μg), AMP (2 mM) or GMP (2 mM), and SHAM (2 mM) or BHAM (2 mM), were added. The *values in parentheses* represent the rate of oxygen uptake and were expressed as ng atoms O/min/5×10^6 cells/ml. *Graphs* are representative of at least three independent assays
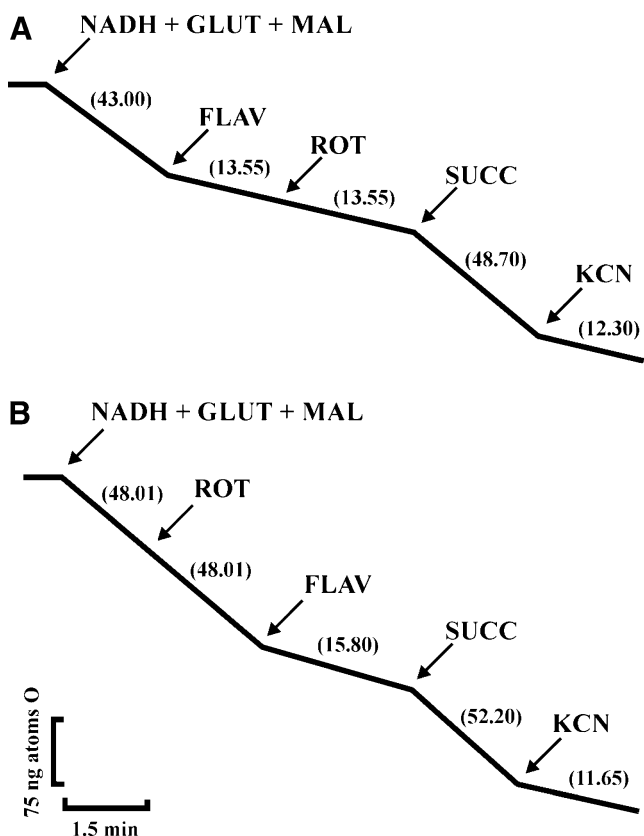
Fig. 3 Exogenous NADH oxidation by *P. brasiliensis* spheroplasts. **a**, **b** Spheroplasts of *P. brasiliensis* (5×10^6 cells per ml) were incubated at 30°C in 1.8 ml of standard incubation medium. At the times indicated by *arrows*, NADH (2 mM), malate (10 mM), glutamate (10 mM), rotenone (40 μM), flavone (500 μM), succinate (10 mM), or KCN (1 mM), were added. The *values in parentheses* represent the rate of oxygen uptake and were expressed as ng atoms O/min/5×10^6 cells/ml. *Graphs* are representative of at least three independent assays

was observed in the $\Delta\psi$, which was completely inhibited after addition of flavone. Although a lower $\Delta\psi$ was observed, a similar pattern occurred in the presence of the Complex I-substrate cocktail without NAD$^+$ (Fig. 5b). After a 96 h growth period, flavone was able to inhibit the $\Delta\psi$ in presence of the same substrate cocktail (Fig. 5c—*a*); two additions of 20 μM rotenone (Fig. 5c—*b*) only slightly affected this state. A similar pattern was observed after 120 h growth (not shown). Following 240 h of growth, a lower $\Delta\psi$ was observed. Although additions of rotenone or flavone alone were unable to inhibit this $\Delta\psi$, it was inhibited when both drugs were added together (Fig. 5d). After 96 h of growth, NADH was able to generate a $\Delta\psi$ (Fig. 5e), which flavone alone was able to inhibit (Fig. 5e—*a*). Rotenone alone could not inhibit the mitochondrial $\Delta\psi$, which was inhibited with further flavone additions (Fig. 5e—*b*). Also, NAD$^+$ was able to generate a $\Delta\psi$ (Fig. 5f), which was slightly lower than that generated by NADH. Flavone alone inhibited this $\Delta\psi$ (Fig. 5f—*a*). However, two additions of rotenone only slightly affected it; and it was fully inhibited

by the subsequent addition of flavone to rotenone-inhibited samples (Fig. 5f—*b*). FCCP is a potent uncoupler that collapses $\Delta\psi$ at very low (1 μM) concentrations. Yet, under our assay conditions, FCCP concentrations as high as 25 μM were required to cause uncoupling. This is probably due to the difficulty of this compound crossing the partially digested cell wall.

To evaluate the contribution of the alternative NADH dehydrogenase or Complex I in each growth phase of *P. brasiliensis* yeast's form, we performed real time-PCR (Fig. 6) using primers for subunit 6 of NADH–Ubiquinone oxidoreductase (Complex I), *nd6Pb* gene, and for the alternative NADH dehydrogenase, *ndhPb* gene. The number of transcripts of *ndhPb* increased from 60 to 96 h of growth, and the number of transcripts of *nd6Pb* increased for up to 48 h and then decreased until 96 h. Following a 240 h growth period, both genes were present in a similar number of transcripts.

Discussion

Digestion of cell walls that does not significantly affect the gross structure and function of intracellular organelles such as mitochondria has been used in studies of various yeast and filamentous fungi (Tudella et al. 2004; Achleitner et al. 1995; Milani et al. 2001b; Monteiro et al. 2004). This technique is particularly useful when the number of cells available is insufficient to proceed using standard mitochondrial isolation procedures or when cells are difficult to
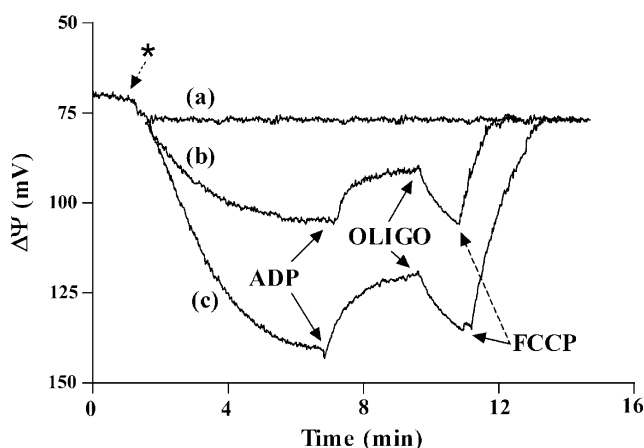

Fig. 4 Mitochondrial membrane potential ($\Delta\psi$) generated by different oxidable substrates. Spheroplasts of *P. brasiliensis* (5×10^6 cells per ml) were incubated at 30°C in 2 ml of standard incubation media. The *arrow* marked with a symbol (*asterisk*) indicates the addition of oxidizable substrates. The oxidizable substrates used were: (*a*) Malate (10 mM), (*b*) Malate/NAD$^+$ (10 mM/2 mM), and (*c*) Succinate (10 mM). At the times indicated by *arrows*, ADP (2 μmol), oligomycin (4 μg), FCCP (25 μM), or KCN (1 mM), were added. *Graphs* are representative of at least three independent assays
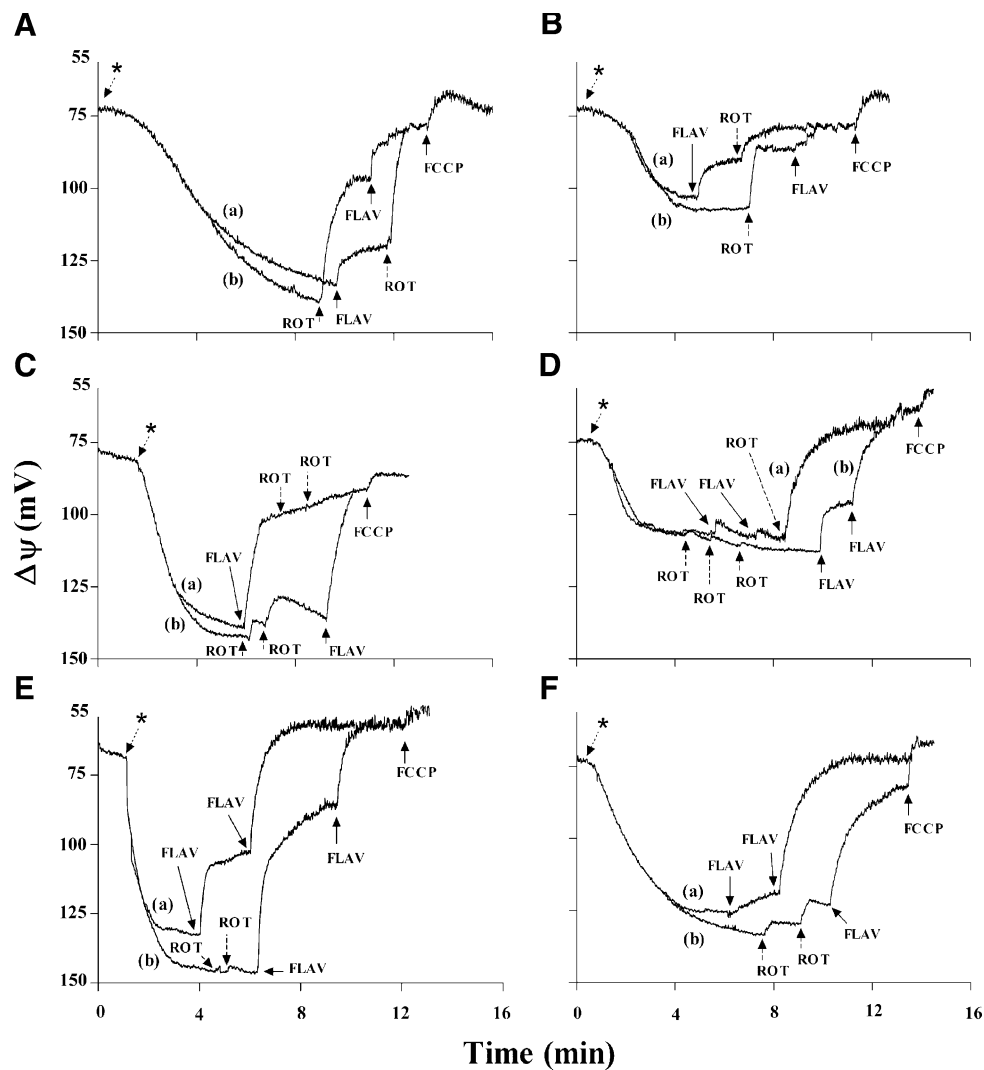
Fig. 5 Influence of cellular growth stage of *P. brasiliensis* on mitochondrial membrane potential and on Complex I and alternative NADH dehydrogenase activities. The experimental conditions are described in the legend of Fig. 4. **a, b** Cells from cultures after 60 h growth; **c, e, f** cells after 96 h growth; **d** cells after 240 h growth. The oxidizable substrates used were: **a, c,** and **d** a mix of malate (10 mM), glutamate (10 mM), citrate (10 mM), pyruvate (10 mM), α-ketoglutarate (10 mM), and NAD$^+$ (2 mM). **b** The same substrate cocktail above without NAD$^+$, **e** NADH (2 mM) and **f** NAD$^+$ (2 mM). (*a*) assays where flavone was added prior to rotenone; (*b*) assays where rotenone was added prior to flavone. At the times indicated by *arrows*, rotenone (40 μM), flavone (500 μM) or FCCP (25 μM), were added. *Graphs* are representative of at least three independent assays

completely homogenize without incurring mitochondrial damage, as is the case for most fungi.

Three groups of NADH:ubiquinone oxidoreductases are known (Kerscher 2000): the proton-translocating NADH: ubiquinone oxidoreductase (designated Complex I in mitochondria and NDH-1 in bacteria), the Na$^+$-translocating NADH:ubiquinone oxidoreductase (only documented in bacteria), and the alternative NADH:ubiquinone oxido-reductase NDH-2, which catalyzes the same redox reaction as does the respiratory chain Complex I, but does not contribute to the generation of a transmembrane proton gradient (Kerscher 2000). In mammalian mitochondria, the NADH dehydrogenase enzyme complex has an intricate structure with at least 43 subunits, a total molecular mass of ~1,000 kDa and is sensitive to rotenone (Walker 1992; Okun et al. 2000; Sazanov and Walker 2000; Kerscher et al. 2001). In contrast, the respiratory chain of *S. cerevisiae* lacks Complex I, having instead three rotenone-insensitive NADH:ubiquinone oxidoreductases: two external rotenone-insensitive NADH:ubiquinone oxidoreductases (Nde1 and Nde2), and one internal rotenone-insensitive NADH:ubi-quinone reductase, Ndi1 (Kerscher 2000). The Ndi1 enzyme of *S. cerevisiae* mitochondria is a single polypep-tide enzyme inhibited by flavone, but not by rotenone. In contrast, the obligate aerobic yeast *Yarrowia lipolytica*, which does have a Complex I, has only one alternative enzyme, encoded by the *ndh2* gene, residing on the external face of the inner mitochondrial membrane (Kerscher et al.
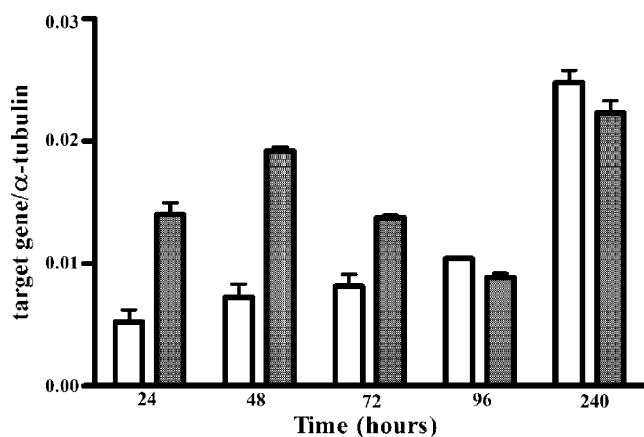
Fig. 6 Expression levels of *ndh*2 (*white bars*) and *nd*6 (*gray bars*) genes after different cellular growth stages of *P. brasiliensis* yeast form. The number of copies of each transcript was determined by Real Time-PCR, as described in experimental procedures, and normalized by the number of copies of α-tubulin transcript. The *graph* is representative of three independent assays

1999). Mitochondria of the filamentous fungus *Neurospora crassa* possess Complex I, as well as three non-proton pumping, alternative NAD(P)H dehydrogenases (Melo et al. 2001; Videira and Duarte 2002).

In most animals, the rotenone and piericidin-sensitive Complex I (Joseph-Horne et al. 2001) provides the sole mechanism for electrons from NADH to enter the respiratory chain; thus, external NADH can be used only via an indirect process or after some degree of damage to the inner mitochondrial membrane. It is relevant to note that mitochondria of *P. brasiliensis* spheroplasts can oxidize exogenous NADH and phosphorylate ADP and that the oxidation of cytoplasmic NADH is not inhibited even by very high concentrations of rotenone, but that it is inhibited by flavone. Flavone derivatives are well-known inhibitors of the external NADH–quinone oxidoreductase of plants (Ravanel et al. 1990). Although high concentrations of rotenone are able to inhibit Complex III and other respiratory enzymes (Teeter et al. 1969), in the present study we have employed this inhibitor at very high concentration because some NADH dehydrogenases are less sensitive to it (Uyemura et al. 2004). Therefore, in addition to the presence of Complex I, our results indicate the presence of an external rotenone-insensitive NADH:ubiquinone oxidoreductase in *P. brasiliensis* mitochondria.

A slight increase in mitochondrial respiration following addition of malate plus NAD$^+$ was observed in *P. brasiliensis* spheroplasts (Table 1). Also, a Δψ inhibition by rotenone or flavone was detected at different growth phases. The ability of NAD$^+$ to generate Δψ could either be related to a recently reported NAD$^+$ transporter in *S. cerevisiae* (NP 012260) (Todisco et al. 2006) or to NADH or succinate

production via the cytosolic malate-dehydrogenase and glyoxylate pathway. This latter pathway has been described as being important during aging in *S. cerevisiae* (Samokhvalov et al. 2004) as well as during phagocytosis in response to nutrient starvation in the phagosomes of opportunistic fungi like *Candida albicans* (Lorenz and Fink 2002). In this context, we have found a sequence in a *P. brasiliensis* gene databank (http://143.107.203.68/pbver2/default.html) with high homology to the NAD$^+$ transporter gene. The *P. brasiliensis* NAD$^+$ transporter peptide has 87% similarity to those of *C. immitis* (XP001244664), 67% to those of *A. fumigatus* (EAL90110.1), 41% to *C. albicans* (XP714565.1), 46% to *Y. lipolytica* (CAG79616.1), 60% to *N. crassa* (XP960808), and 45% to *S. cerevisiae* (YIL006W). This suggests that the *P. brasiliensis* gene plays the same role as that characterized for *S. cerevisiae*.

The rates of oxidation of NADH-linked substrates, as well as the effect of NAD$^+$, appear to be influenced by the stage of growth of *P. brasiliensis*. The sensitivity to rotenone observed in the early phase (60 h) decreased markedly in the late exponential stage (120 h), in contrast to the effect of flavone, which remained during the stationary phase (240 h). This suggests a greater participation of the alternative NADH dehydrogenase during the stage of exponential growth of *P. brasiliensis*, confirmed by the fact that during this stage the number of copies of the *nd6Pb* gene decreased, in contrast to the observed increase in the number of copies of *ndhPb*.

The increased oxygen uptake in the presence of ADP was stimulated by succinate, indicating the presence of the respiratory chain Complex II in mitochondria of *P. brasiliensis*. The partial inhibition of respiration by antimycin A and KCN indicates the presence of the ubiquinol–cytochrome *c* oxidoreductase (complex III) and of cytochrome *c* oxidase (Complex IV); the inhibition of state 3 respiration by oligomycin demonstrates the presence of ATP synthase (Complex V). The inhibition of *P. brasiliensis* KCN-resistant respiration by BHAM or SHAM, as well as its stimulation by GMP or AMP, reveals the presence of an alternative oxidase, branching out at the ubiquinone level of the respiratory chain, and bypassing two sites of energy conservation in the cytochrome pathway. Similar alternative oxidases have been documented in many fungi including *C. parapsilosis* (Guerin and Camougrand 1986; Milani et al. 2001a), *H. capsulatum* (Maresca et al. 1981), *A. niger* (Kirimura et al. 1996), *N. crassa* (Li et al. 1996), *C. albicans* (Huh and Kang 2001), and *A. fumigatus* (Tudella et al. 2004). Most of these fungi are exposed to oxidative stress by reactive oxygen or nitrogen species produced by polymorphonuclear leukocytes and alveolar macrophages (Brummer et al. 1989; Moreira et al. 2004). The alternative oxidases may enable them to tolerate hostile environments and allow them to survive inside the

phagolysosomes of macrophages. Some antioxidant enzymes present in aerobic organisms eliminate toxic oxygen radicals, thereby contributing to survival (Marques et al. 2004; Moreira et al. 2004). The damage caused by oxidative stress or the production of reactive oxygen species can be reduced by other mechanisms, which depend on enzymes like mitochondrial alternative oxidase (Berthold et al. 2000) or on other fungal alternative respiratory pathways (Joseph-Horne et al. 2001).

The current study documents the presence of alternative respiratory chain pathways in addition to Complex I, as well as the capacity to utilize NADH-linked substrates, in *P. brasiliensis* mitochondria. It appears reasonable, therefore, to suggest that *P. brasiliensis* is, in principle, potentially susceptible to a wide range of pharmacological agents to target mitochondria.

References

Achleitner G, Zweytick D, Trotter PJ, Voelker DR, Daum G (1995) J Biol Chem 270:29836–29842

Akerman KE, Wikstrom MK (1976) FEBS Lett 68:191–197

Berthold DA, Andersson ME, Nordlund P (2000) Biochim Biophys Acta 1460:241–254

Borecky J, Vercesi AE (2005) Biosci Rep 25:271–286

Brummer E, Hanson LH, Restrepo A, Stevens DA (1989) Infect Immun 57:2289–2294

Brummer E, Castaneda E, Restrepo A (1993) Clin Microbiol Rev 6:89–117

Chance B, Williams GR (1956) Adv Enzymol Relat Subj Biochem 17:65–134

Franco M (1987) J Med Vet Mycol 25:5–18

Goldman GH, dos Reis Marques E, Duarte Ribeiro DC, de Souza Bernardes LA, Quiapin AC, Vitorelli PM, Savoldi M, Semighini CP, de Oliveira RC, Nunes LR, Travassos LR, Puccia R, Batista WL, Ferreira LE, Moreira JC, Bogossian AP, Tekaia F, Nobrega MP, Nobrega FG, Goldman MH (2003) Eukaryot Cell 2:34–48

Guerin M, Camougrand N (1986) Eur J Biochem 159:519–524

Harman D (1956) J Gerontol 11:298–300

Harman D (1981) Proc Natl Acad Sci USA 78:7124–7128

Harman D (1998) J Int Fed Clin Chem 10:24–27

Helmerhorst EJ, Murphy MP, Troxler RF, Oppenheim FG (2002) Biochim Biophys Acta 1556:73–80

Huh WK, Kang SO (2001) Biochem J 356:595–604

Jarmuszkiewicz W, Behrendt M, Navet R, Sluse FE (2002) FEBS Lett 532:459–464

Jezek P, Hlavata L (2005) Int J Biochem Cell Biol 37:2478–2503

Johnson CH, Prigge JT, Warren AD, McEwen JE (2003) Yeast 20:381–388

Joseph-Horne T, Hollomon DW, Wood PM (2001) Biochim Biophys Acta 1504:179–195

Kerscher SJ (2000) Biochim Biophys Acta 1459:274–283

Kerscher SJ, Okun JG, Brandt U (1999) J Cell Sci 112(Pt 14):2347–2354

Kerscher SJ, Eschemann A, Okun PM, Brandt U (2001) J Cell Sci 114:3915–3921

Kirimura K, Matsui T, Sugano S, Usami S (1996) FEMS Microbiol Lett 141:251–254

Kowaltowski AJ, Cosso RG, Campos CB, Fiskum G (2002) J Biol Chem 277:42802–42807

Li Q, Ritzel RG, McLean LL, McIntosh L, Ko T, Bertrand H, Nargang FE (1996) Genetics 142:129–140

Lorenz MC, Fink GR (2002) Eukaryot Cell 1:657–662

Maresca B, Lambowitz AM, Kumar VB, Grant GA, Kobayashi GS, Medoff G (1981) Proc Natl Acad Sci USA 78:4596–4600

Marques ER, Ferreira ME, Drummond RD, Felix JM, Menossi M, Savoldi M, Travassos LR, Puccia R, Batista WL, Carvalho KC, Goldman MH, Goldman GH (2004) Mol Genet Genomics 271:667–677

Medoff G, Painter A, Kobayashi GS (1987) J Bacteriol 169:4055–4060

Melo AM, Duarte M, Moller IM, Prokisch H, Dolan PL, Pinto L, Nelson MA, Videira A (2001) J Biol Chem 276:3947–3951

Milani G, Jarmuszkiewicz W, Sluse-Goffart CM, Schreiber AZ, Vercesi AE, Sluse FE (2001a) FEBS Lett 508:231–235

Milani G, Schereiber AZ, Vercesi AE (2001b) FEBS Lett 500:80–84

Monteiro G, Kowaltowski AJ, Barros MH, Netto LE (2004) Arch Biochem Biophys 425:14–24

Moreira SF, Bailao AM, Barbosa MS, Jesuino RS, Felipe MS, Pereira M, de Almeida Soares CM (2004) Yeast 21:173–182

Okun JG, Zickermann V, Zwicker K, Schagger H, Brandt U (2000) Biochim Biophys Acta 1459:77–87

Petrussa E, Braidot E, Nagy G, Vianello A, Macri F (1992) FEBS Lett 307:267–271

Ramos ESM, Saraiva LES (2008) Dermatol Clin 26:257–269, vii

Ravanel P, Creuzet S, Tissut M (1990) Phytochemistry 29:441–445

Restrepo A (1985) Sabouraudia 23:323–334

Restrepo A, McEwen JG, Castaneda E (2001) Med Mycol 39:233–241

Samokhvalov V, Ignatov V, Kondrashova M (2004) Biochimie 86:39–46

San-Blas F, San-Blas G, Gil F (1994) J Med Vet Mycol 32:381–388

San-Blas G, Nino-Vega G, Iturriaga T (2002) Med Mycol 40:225–242

Sazanov LA, Walker JE (2000) J Mol Biol 302:455–464

Semighini CP, de Camargo ZP, Puccia R, Goldman MH, Goldman GH (2002) Diagn Microbiol Infect Dis 44:383–386

Siedow JN, Umbach AL (1995) Plant Cell 7:821–831

Suzuki T, Hashimoto T, Yabu Y, Majiwa PA, Ohshima S, Suzuki M, Lu S, Hato M, Kido Y, Sakamoto K, Nakamura K, Kita K, Ohta N (2005) J Eukaryot Microbiol 52:374–381

Teeter ME, Baginsky ML, Hatefi Y (1969) Biochim Biophys Acta 172:331–333

Tischner R, Planchet E, Kaiser WM (2004) FEBS Lett 576:151–155

Todisco S, Agrimi G, Castegna A, Palmieri F (2006) J Biol Chem 281:1524–1531

Tudella VG, Curti C, Soriani FM, Santos AC, Uyemura SA (2004) Int J Biochem Cell Biol 36:162–172

Uyemura SA, Luo S, Vieira M, Moreno SN, Docampo R (2004) J Biol Chem 279:385–393

Vanlerberghe GC, McIntosh L (1997) Annu Rev Plant Physiol Plant Mol Biol 48:703–734

Veiga A, Arrabaca JD, Loureiro-Dias MC (2003) FEMS Yeast Res 3:239–245

Videira A, Duarte M (2002) Biochim Biophys Acta 1555:187–191

Walker JE (1992) Q Rev Biophys 25:253–324